Deep–Sea Research II 202 (2022) 105123

Contents lists available at ScienceDirect

Deep-Sea Research Part II

journal homepage: www.elsevier.com/locate/dsr2

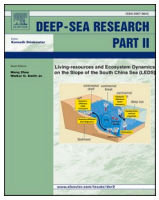

The paralarval stage as key to predicting squid catch: Hints from a process-based model

Jorn Bruggeman [a,b,*], Zoe L. Jacobs [c], Ekaterina Popova [c], Warwick H.H. Sauer [d], Jessica M. Gornall [d], Robert J.W. Brewin [e], Michael J. Roberts [c,f]

[a] Bolding & Bruggeman ApS, Asperup, Denmark
[b] Plymouth Marine Laboratory, United Kingdom
[c] National Oceanography Centre, Southampton, United Kingdom
[d] Department of Ichthyology and Fisheries Science, Rhodes University, Makhanda, South Africa
[e] Centre for Geography and Environmental Science, College of Life and Environmental Sciences, University of Exeter, Penryn Campus, Cornwall, United Kingdom
[f] Nelson Mandela University, Port Elizabeth, South Africa

ARTICLE INFO

Keywords:
Chokka squid
Size spectra
Dynamic energy budget models
Paralarvae
Catch prediction
Agulhas bank

ABSTRACT

Squid species show pronounced interannual variability in population size. While this may partially reflect changes in fisheries pressure, it is thought to be primarily the result of environmental variability. Most squid have an annual life cycle with only a short period dedicated to reproduction. With little overlap between generations, the environment can exert a major influence on stock size. In this study we explore, through a combination of process-based modelling and statistical analysis, whether environmental variability explains variability in catch of the chokka squid, *Loligo reynaudii*, over the Agulhas Bank off South Africa. We focus on growth and survival during the first two months spent as "paralarva" in the pelagic. This period has been suggested to be a key bottleneck and a potential predictor of catch. To describe prey availability and predation pressure, we develop a dynamic model of the size spectrum (1 mg–1000 kg) of the ecosystem over the Agulhas Bank, with trophic interactions governed by size. In tandem, we develop a model for the growth of individual *L. reynaudii*, which specifies where in the size spectrum individual squid can be found at each stage of their development. We find a correlation of 0.74 between modelled biomass representative for *L. reynaudii* at the end of its paralarval stage and catch per unit effort (CPUE) in the subsequent season in the period 1995–2015. This suggests that the paralarval stage is indeed a bottleneck: modelled food availability and predation pressure experienced by paralarvae explains 55% of the variability in CPUE, which is a proxy for spawning stock biomass. As the paralarval stage ends approximately nine months before the time of spawning and maximum catch, this work could be used to develop catch predictor with a nine-month lag.

1. Introduction

Cephalopods such as squid, cuttlefish and octopus are highly effective predators and play a key role in marine ecosystems. They reach sizes comparable to fish but have a life cycle that is compressed into just 1–2 years. Their strategy has been described as "live fast, die young" (Boyle and Rodhouse, 2005) and, in squid, "life in the fast lane" (Jackson and O'Dor, 2001): they grow fast, often reproduce just once, and die soon after. Without the multiple overlapping generations found in fish, cephalopod populations are thought to be particularly sensitive to environmental fluctuations (Pierce et al., 2008, 2010). Accordingly, their stocks show pronounced interannual variability. This is reflected in fisheries landings where it has become more obvious as cephalopods have been increasingly targeted (Hunsicker et al., 2010), with evidence suggesting that stocks may already be subject to overexploitation (Rodhouse et al., 2014). However, such trends are difficult to diagnose in the presence of pronounced natural variability in stock size. There is thus an urgent need to understand and predict this variability, and numerous studies have attempted to do this (e.g., Moustahfid et al., 2021; Rodhouse et al., 2014).

The extensively studied chokka squid, *Loligo reynaudii*, displays many of the features attributed to the archetypical cephalopod. It is found

* Corresponding author. 43 Rosslyn Park Road, Plymouth, PL3 4LL, UK.
E-mail address: jorn@bolding-bruggeman.com (J. Bruggeman).

https://doi.org/10.1016/j.dsr2.2022.105123
Received 2 July 2021; Received in revised form 26 May 2022; Accepted 1 June 2022
Available online 22 June 2022

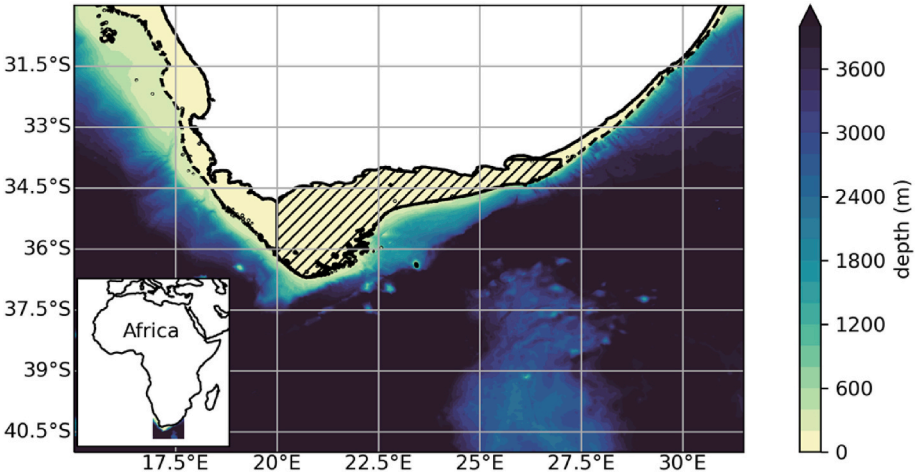

Fig. 1. Map of the south coast of South Africa, showing the Agulhas Bank where *L. reynaudii* is typically found. The 200 m depth contour that delineates the bank is shown as dashed line. The model developed in the methods section is restricted to the central and eastern parts of the bank, shown as hatched area. Depths were taken from GEBCO 2020 (GEBCO Compilation Group, 2020).

along a substantial portion of the coast of South Africa, but particularly over the Agulhas Bank (AB) which covers an area of 29,000 square nautical miles (Fig. 1). Squid appear to live and grow across the Bank before migrating back to near-coastal spawning grounds; the proposed life cycle can be found in Lipiński et al. (2016). *L. reynaudii* is a species of commercial importance (Cochrane et al., 2014), with fisheries primarily targeting spawning aggregations in relatively shallow water (<50 m) in summer (Sep–Dec).

As for many cephalopods, the stock size of *L. reynaudii* is highly variable. In fact, "the chokka squid fishery has the highest variability in both biomass and catches of all the South African commercial fisheries" (Sauer et al., 2013). Unsurprisingly, fluctuating stock raises concerns of overexploitation, particularly in years of poor recruitment. The sustainability of the fisheries has been discussed for nearly 30 years (Augustyn et al., 1992) and measures to prevent overexploitation, including effort capping and seasonal closure, are in place (Roel and Butterworth, 2000). However, much of the variability in *L. reynaudii* stock is thought to be due to the environment, e.g., near-bottom turbidity, temperature and oxygen at the time of spawning (Roberts and Sauer, 1994) and changes in circulation and their impact on early life stages (Downey-Breedt et al., 2016; Martins et al., 2014). A predictive model linking environment and catch was proposed by Roberts (2005) who found a statistical relationship between catch and summer sea surface temperature. However, this relationship degraded when updated with data from recent years (Sauer et al., 2013). Similarly, Jebri et al. (2022) found a statistical relationship between catch and chlorophyll *a* concentration on the bank, with the latter being controlled primarily by changes in wind.

As explanations for variability in *Loligo reynaudii* tend to focus on specific phases in its life history (e.g., spawning, hatching, early development), we briefly review the characteristic features of its growth, reproduction, and survival. *L. reynaudii* grows from 2 mg wet mass at hatching (Martins et al., 2010; Vidal et al., 2005) to between 200 g (females) and 400 g (males) at spawning, with some males ultimately reaching 1 kg (Augustyn, 1990). Wet mass increases over five orders of magnitude in approximately one year. Much of the growth happens early: cephalopods grow exponentially early in life, but slower after (Boyle and Rodhouse, 2005; Forsythe and van Heukelem, 1987; Lipiński, 2002). This is characteristic for *L. reynaudii* as well: different developmental phases are thought to have very different growth rates (Sauer et al., 2013), with growth after hatching typically described with an exponential relationship (Vidal et al., 2005). Reproduction is thought to take place after one year, with 8,000 to 17,000 eggs (Sauer et al., 1999) being deposited during several spawning episodes (Melo and Sauer, 2007). There is no evidence for mass mortality directly after spawning but longevity is thought not to exceed 18 months, with 15 months being a commonly suggested expected lifespan (Augustyn et al., 1994; Augustyn and Roel, 1998). Evidence suggests that the life cycle is at least partially synchronized with the seasons, with a major spawning peak in spring and early summer (Sep–Dec) and an occasional minor peak in autumn or winter (Mar–Jul) (Augustyn et al., 1994; Olyott et al., 2007). Further indications that early summer is the main time of spawning are given by the pronounced decrease in the number of viable oocytes per female *L. reynaudii* during this period (Melo and Sauer, 1998), and the fact that fisheries, which target spawning aggregations, simultaneously show a maximum in catch (Sauer et al., 2013).

The life of cephalopods is punctuated by several key transitions (Robin et al., 2014). For squid such as *L. reynaudii*, perhaps most important of these is the transition from pelagic paralarva to a final demersal-by-day, pelagic-by-night lifestyle, dominated by diel vertical migration. While this transition is foremost an ecological one, describing a difference in habitat and behaviour (von Boletzky, 2003), it is not just that: the end of the paralarval stage coincides with changes in morphology and growth (Robin et al., 2014; Shea and Vecchione, 2010; Young and Harman, 1988). In fact, the original paper introducing the "paralarva" already states that it is separated from the subadult by "distinct early discontinuities in growth patterns" (Young and Harman, 1988). This is important as it implies that it may be possible to infer the time of change in habitat, behaviour and ecology associated with the end of the paralarval stage from the growth curve, and vice versa – a feature we exploit in this study.

The paralarval stage is thought to be a potential bottleneck in the life cycle of *L. reynaudii*. As paralarvae use their limited swimming ability primarily to maintain their position in the water column (Augustyn et al., 1994), their horizontal location is dictated by ocean currents. Thus, the availability of their food (small crustaceans) is the combined result of currents and the productivity of the local plankton food web. Food availability becomes critical three to five days after hatching (Martins et al., 2010; Vidal et al., 2005) and likely remains so during the remaining months spent as paralarva. Accordingly, the paralarval stage is a time during which the physical and biological environment can exert a disproportionate influence on growth and survival. It is also a time during which predation pressure is high: for *Loligo vulgaris*, paralarval mortality in the field was estimated at 4.8–9.6% per day (González et al., 2010). Based on these numbers, survival at the end of the paralarval stage, which lasts three months in this species, would range between 0.02% and 1%.

Food availability and predation pressure follow from trophic

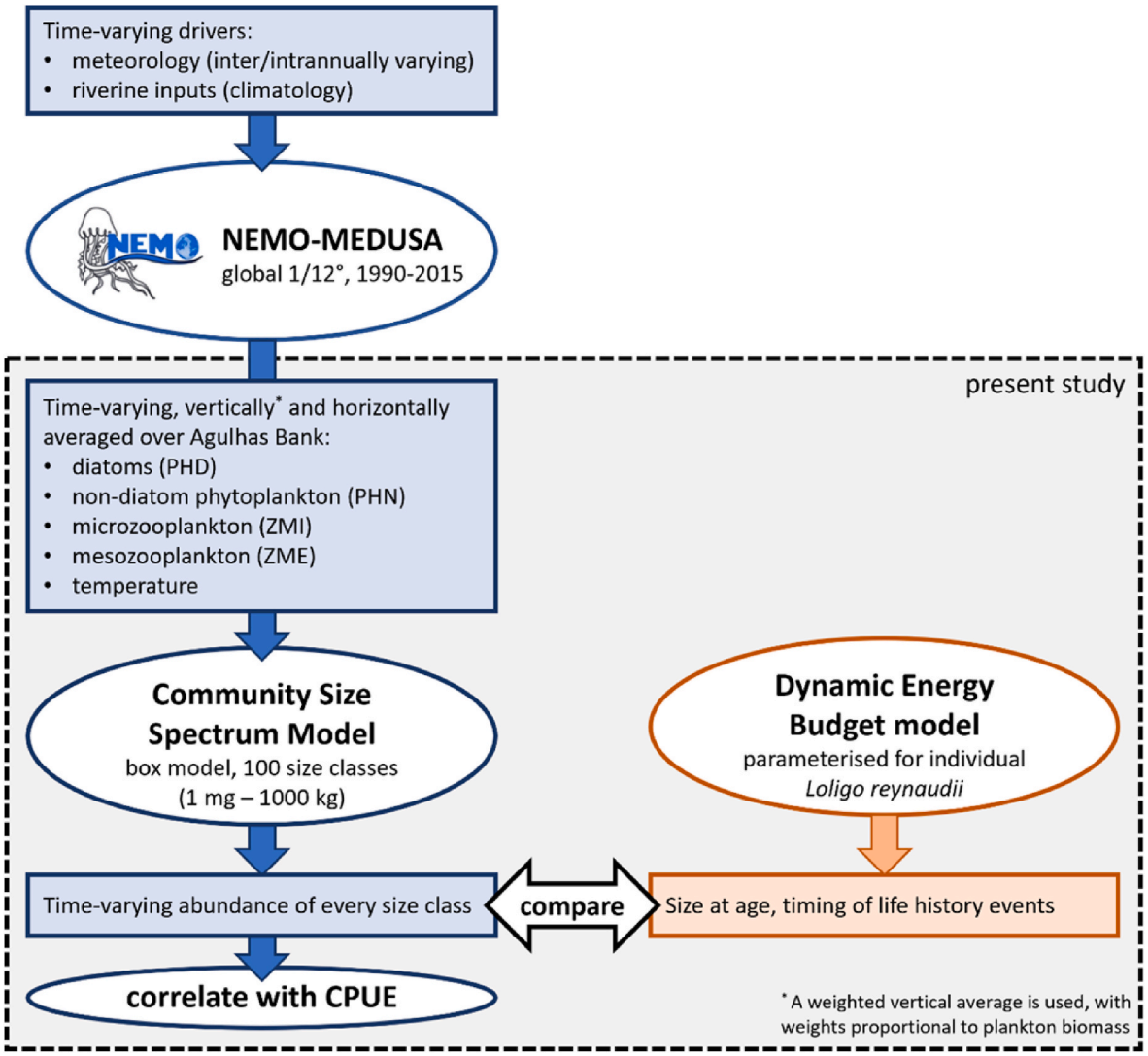

Fig. 2. Overview of all model components and the data they exchange. The rectangle labelled "present study" encompasses all models and analyses that are run as part of this study. They are driven by pre-existing outputs from the NEMO-MEDUSA model, shown outside the rectangle.

relationships which are thus major factors ultimately determining cephalopod population size and catch (Rodhouse et al., 2014). These relationships change during ontogenetic development. Like most marine species, *L. reynaudii* and its predators are opportunistic, feeding on prey proportional to their own body size (Lipiński, 1992). Accordingly, prey preference of *L. reynaudii* varies with size and age: young paralarvae feed on small crustaceans such as calanoid copepods (Venter et al., 1999), juveniles on larger crustaceans (e.g., euphausiids) and larval fish (Lipiński, 1987), adults on large crustaceans (e.g., various species of shrimp), fish and cephalopods, with cannibalism being an important factor (Sauer and Lipiński, 1991). After the onset of diel vertical migration, benthic species (decapods, demersal fish) make up an important part of the diet (Lipiński, 1987). Quantitative estimates of predator-prey size ratios for squid are rarely available and sometimes inconclusive (Boyle and Rodhouse, 2005; Rodhouse and Nigmatullin, 1996), though Vovk (1985) shows *Loligo palei* prefers prey that measures 8–20% of its own mantle length.

Similar size-based rules likely govern the prey preference of potential predators of *L. reynaudii*. If so, it is exposed to predation by ever larger predator species as it grows. However, empirical observations of predation on *L. reynaudii* are limited to spawning aggregations, and thus, adults. These are predated upon by cephalopods, teleosts, chondrichthyans and marine mammals (Smale et al., 2001). Predation on smaller individuals is generally not observed, with the ecology of paralarvae, in particular, remaining an important knowledge gap (Sauer et al., 2013). Still, given the large number of species involved in *L. reynaudii* predation, generic rules for predator-prey preference are likely to apply, e.g., a typical mass ratio between predator and its *L. reynaudii* prey that ranges between 100 and 1000 (Jennings et al., 2002).

In this study we explore the extent to which food availability and predation pressure during the paralarval stage of *L. reynaudii* can explain variability in catch per unit effort (CPUE), which we interpret as proxy of population size. We use a combination of models to investigate this (Fig. 2). First, we construct a dynamic model for the pelagic size spectrum (Blanchard et al., 2009; Cheung et al., 2018) over the Agulhas Bank. This model describes the temporal variation in biomass in 100 size classes ranging from 1 mg to 1000 kg and centres on size-based trophic interactions. It is driven by existing outputs of a 1/12° coupled hydrodynamic-biogeochemical model, NEMO-MEDUSA (Yool et al., 2013). Second, we develop a bioenergetic model (Kooijman, 2010), describing the life history of individual *L. reynaudii*, and constrain this with empirical observations of egg development, paralarval growth, adult lifespan and fecundity. Predicted growth curves from this model are used to determine where in the size spectrum paralarvae are positioned at each stage of their development. We compute correlations

between CPUE and outputs of the size spectrum model (abundance per size class) throughout the year. Using the bioenergetic model, the resulting patterns are interpreted in terms of implications for the life history of *L. reynaudii* and its impact on catch.

2. Methods

2.1. Modelling the size structure of the Agulhas Bank ecosystem

To describe the time-varying size structure of the marine ecosystem over the Agulhas Bank, we use a recent implementation (https://doi.org/10.5281/zenodo.4593394) of the Community Size Spectrum Model (CSSM, Blanchard et al., 2009). At its core, this is a box model that is typically applied to large areas such as the North Sea (Blanchard et al., 2009) or entire Exclusive Economic Zones (Blanchard et al., 2012; Cheung et al., 2018). Here we use it to describe the pelagic ecosystem over the Agulhas Bank, defined as all waters with a depth shallower than 200 m in the area spanning 33.8–37 °South, 20–27 °East (Fig. 1). Within this area the model is horizontally averaged.

The equations describing the processes in the size spectrum model have been published previously (Blanchard et al., 2009, 2014); the specific model configuration matches earlier work (Cheung et al., 2018) and is summarized here. The model represents depth-integrated wet mass (g/m^2) in individuals between 1 mg and 1000 kg, partitioned over 100 log-spaced size classes. Unlike Blanchard et al. (2009), we model the pelagic size spectrum only as we focus exclusively on the pelagic life stage of *L. reynaudii*. Benthic fauna and demersal fish are therefore not included. Trophic interactions are governed by size-based preferences, which are characterised by a log-normal distribution of prey size centred at an optimal (median) predator: prey mass ratio of 100 (Blanchard et al., 2009; Hartvig et al., 2011; Scott et al., 2014). The standard deviation of this distribution is 1 $\log^{10}$ g. Food ingestion is further controlled by a clearance rate (volume predator^{-1} time^{-1}) that is size-dependent: large predators search larger volumes of water per unit time. All rates are temperature-dependent with an activation energy of 0.63 eV (Blanchard et al., 2012; Cheung et al., 2018). The gross growth conversion efficiency of ingested prey to predator biomass is set to 0.2 (Blanchard et al., 2009). This combines the assimilation efficiency (the fraction of ingested food that is successfully assimilated, as opposed to egested) and the loss of assimilated mass/energy to metabolic processes. Fishing is prescribed as a fixed mortality of 0.4 yr^{-1} for individuals above 1.25 g. This threshold was selected to account for catch for human consumption as well as fish meal production (Blanchard et al., 2012). Production of new individuals in the smallest size class (1 mg) is not controlled by stock-recruitment relationships but by continuously setting the biomass in lowest size class to an expected biomass obtained by extrapolating the plankton size spectrum (Woodworth-Jefcoats et al., 2013). The model thus assumes the smallest sizes of predators will appear wherever and whenever prey for them is available.

To provide prey for the smallest size classes in the CSSM, we prescribe the (time-varying) concentration of organisms smaller than the minimum resolved size of 1 mg. These smaller organisms include all unicellular plankton (bacteria, phytoplankton, microzooplankton) and most multicellular zooplankton. These fields are taken from a 1/12° global simulation with the NEMO-MEDUSA coupled hydrodynamic-biogeochemical model (Yool et al., 2013). While this simulation covers the period 1990–2015, we only use results from 1995 onwards to ensure the model has reached quasi-equilibrium with a repeating annual cycle in productivity. We infer the plankton spectrum from the concentration (mmol N/m^3) of each of the four MEDUSA plankton functional types (PFTs): diatoms, non-diatom phytoplankton, microzooplankton, and mesozooplankton. Each is assumed to span a fixed wet mass range: 4.2 pg–4.2 ng for non-diatom phytoplankton (corresponding to 2–20 μm ESD for a cell density of 1 g/cm^3), 4.2 ng–4.2 μg for diatoms and microzooplankton (20–200 μm ESD), and 10 μg–1 mg for mesozooplankton (Andrew Yool, pers comm, 2018). The total biomass of each PFT is assumed to be uniformly distributed over log-spaced wet mass, corresponding to a Sheldon-Sutcliffe size spectrum (Sheldon et al., 1972). Wet mass is obtained from nitrogen by multiplying each concentration with MEDUSA's C: N ratio (6.625 for phytoplankton, 5.625 for zooplankton; Yool et al., 2013) and an assumed wet: carbon mass ratio of 10 (Boudreau and Dickie, 1992). The combined plankton spectrum spans 4.2 pg to 1 mg in wet mass with 84 log-spaced size classes.

The treatment of depth in the model merits separate discussion. The larger organisms described by the size spectrum model in reality control their vertical position in the water column and may adjust it dynamically to prey availability and predator presence, e.g., through diel vertical migration. This is not easily represented in a model of the entire pelagic community; it typically requires additional assumptions and explicit treatment of functional guilds (van Denderen et al., 2021). For the sake of simplicity, we assume instead that all the pelagic predators redistribute instantaneously in the vertical according to prey availability (Cheung et al., 2018). Since all modelled predators prefer smaller prey, this assumption causes predator concentrations at any depth to be proportional to the smallest prey: the sum of all plankton biomass at that depth. This applies for any size of predator. The resulting vertical predator distribution $c(z)$ can be summarized by the interaction depth, $[\int c(z)dz]^2 / \int c^2(z)dz$, which represents the effective depth range over which predator-prey interactions within the predator community occur. As this metric depends on plankton, it will vary over time: the depth distribution of predators will dynamically expand and contract, similar to mixed layer models for plankton (Evans and Parslow, 1985). While this treatment of depth distribution is relatively simple, it nonetheless accounts for the restricted and seasonally varying depth extent of the energy at the base of the food web; as such, we consider it preferable over approaches that distribute predators over a prescribed constant depth or over the entire water column. The time-varying depth distribution is computed from NEMO-MEDUSA outputs and is subsequently used to weigh depth-resolved concentrations of plankton when computing their depth-averaged concentration. The interaction depth generally ranges between 45 m (summer) and 85 m (winter) over the Agulhas Bank.

In addition to plankton, a weighted depth average of temperature is derived from NEMO-MEDUSA outputs. This is, once again, a weighted-depth average based on the depth distribution of predators described in the previous section. For both plankton and temperature, depth-averaged values are extracted per model grid box (1/12° × 1/12°) and subsequently averaged over the aforementioned "Agulhas Bank" target area.

The size spectrum model is configured to run at a daily time step to fully resolve both seasonal and interannual time scales which are central to the question of catch variability in *L. reynaudii*. It should be noted that size spectrum models are more commonly used to assess steady state distributions or long-term variability on annual times scales (Blanchard et al., 2012). However, there is precedent for using size spectrum models at seasonal time scales (Datta and Blanchard, 2016). NEMO-MEDUSA outputs are available at 5 d resolution and are linearly interpolated during simulation with the size spectrum model.

2.2. A bioenergetic model for the life cycle of L. reynaudii

To relate predicted abundance per size class to the life history of *L. reynaudii*, we need an estimate of its wet mass at any given point during its life cycle. To this end, we construct a Dynamic Energy Budget (DEB) model (Kooijman, 2010) for *L. reynaudii*. This model describes growth, reproduction and survival from fertilization until death. It distinguishes several key life history events, including the start of feeding, an optional "metamorphosis" which we equate with the end of the paralarval stage (see next section), and the start of reproduction. The DEB model has a total of 13 parameters and, as such, is more complex

than many existing cephalopod growth models (Arkhipkin and Roa-Ureta, 2005; Grist and Jackson, 2004; Lipiński, 2002; O'Dor et al., 2005). However, it has the distinct benefit of covering the entire life cycle, not just growth or maturity and fecundity (Macewicz et al., 2004). As a result, its parameters can be constrained with a wide range of observations from any life stage. The model also inherently accounts for the effect of food level and temperature on every aspect of life history.

We use the "abj" extension of the standard DEB model (Kooijman, 2014) which allows for a period of fast exponential growth directly after the start of feeding. This matches the initial exponential growth phase exhibited by most cephalopods (Forsythe and van Heukelem, 1987). In the model, the exponential phase ends at "metamorphosis", after which growth conforms to the von Bertalanffy equation if food availability is constant. Thus, the model can capture the characteristic two-phase growth of cephalopods (Boyle and Rodhouse, 2005). It should be noted that DEB parameters for cephalopods are generally chosen such that the asymptotic size implied by the von Bertalanffy equation is never reached; instead, individuals grow rapidly until (programmed) death, which typically occurs long before growth would saturate (Kooijman, 2010). Nevertheless, some slowing down of growth around the time of maturation can still be seen in these models which qualitatively agrees with a third, slower growth phase (Lipiński, 2002) that has been proposed for *L. reynaudii* (Sauer et al., 2013).

In the DEB model, hatching by default coincides with the start of feeding. This does not apply to paralarvae of *L. reynaudii*: they are not fully developed when they hatch and survive on the remainder of the yolk for the first three to five days (Vidal et al., 2005). During this period, they do not feed. To represent this, we introduce a new parameter for maturity at hatching. This parameter does not affect the behaviour of the model but allows us to align model predictions with experimental results defined relative to the time of hatching (Oosthuizen et al., 2002; Vidal et al., 2005). By defining hatching by a maturity threshold (as opposed to, e.g., a fixed number of days before the start of feeding), we can directly account for the influence of temperature and the initial energy content of eggs on both the time of hatching and the time delay between hatching and feeding. It also implies that while the time of hatching is temperature-dependent, the state of the newly hatched paralarva (e.g., yolk content) is not. This agrees with observations (Martins et al., 2010).

Every aspect of the behaviour of DEB models is directly or indirectly influenced by food availability which is measured by the value of the functional response f (0–1). In the absence of detailed information about this variable, we use $f = 0.6$ when simulating growth and development of *L. reynaudii* in the field; this value is thought to represent the average food level across the marine ecosystem (Hartvig et al., 2011). A different value of $f = 1$ is used while calibrating the DEB model against results from paralarval growth experiments (Vidal et al., 2005) to account for the fact that these experiments were conducted at replete food.

A Bayesian approach (Haario et al., 2001) is used to parameterise the model. First, a multivariate prior distribution is obtained through phylogenetic inference (https://deb.bolding-bruggeman.com, Bruggeman et al. subm., Bruggeman et al., 2009). This approach estimates DEB parameters from a dataset of DEB models for over 2000 parameterised species (https://debtheory.fr/add_my_pet/, Marques et al., 2018), including 19 cephalopods. The inferred prior distribution is combined with several observational datasets specific to *L. reynaudii* to derive the posterior probability of DEB parameters. The following datasets are used:

- Duration of egg development at different temperatures (Oosthuizen et al., 2002)
- Growth of paralarvae in the first 22 days since hatching (Vidal et al., 2005)
- A wet mass between 200 g (female) and 400 g (male) at an age of one year (Augustyn, 1990)
- An expected lifespan of 15 months (Augustyn et al., 1994)

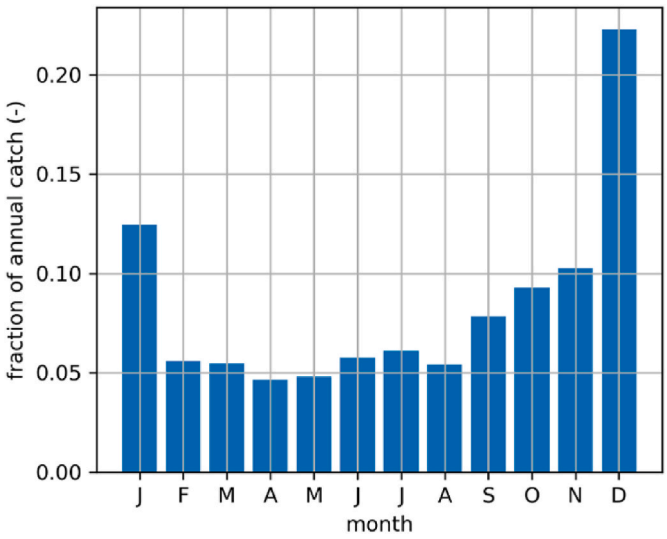

Fig. 3. Monthly catch of the squid *L. reynaudii* as fraction of total annual catch. The annual catch is computed as centred running total, i.e., for each time point, the corresponding total is computed by taking the sum over all catches from 6 months before to 6 months after. Each bar represents the average value between 1990 and 2016.

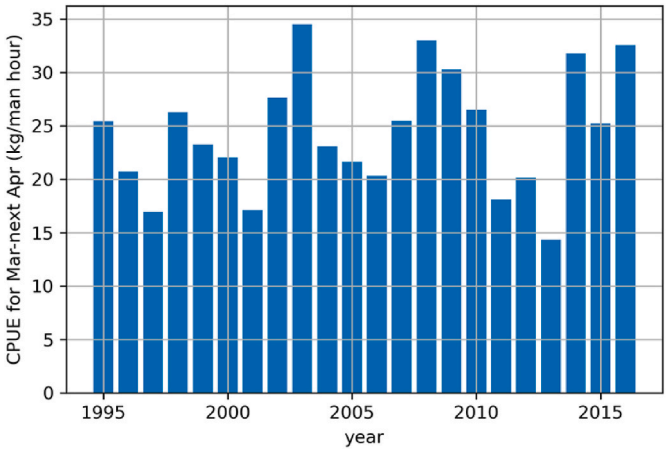

Fig. 4. *L. reynaudii* catch per unit effort between 1995 and 2016. Each annual value represents the period covering April until March the following year to ensure it fully encompassed a single spawning/catch season (Nov–Jan).

- A maximum lifetime reproductive output of 17,000 (Sauer et al., 1999). This is taken to be achieved at an age of 18 months (Augustyn and Roel, 1998). It is worth noting that as this age exceeds the expected lifespan, it will be reached by a minority of individuals only.

The posterior probability is characterised by an ensemble of 500,000 parameter sets. For each of these, time series of growth, reproduction and survival over an 18-month period are simulated. In these simulations, temperature is set to 17.3°C (the long-term average of temperature in the size-spectrum model for the AB) and food availability was set to $f = 0.6$ (Hartvig et al., 2011). Results are visualized as the 2.5, 25, 50, 75, 97.5 percentiles of these 500,000 simulations.

2.3. From size spectra to catch

2.3.1. Catch per unit effort

Total catch of *L. reynaudii* and man hours fished for 1995–2017 were obtained from the South African Department of Forestry, Fisheries and

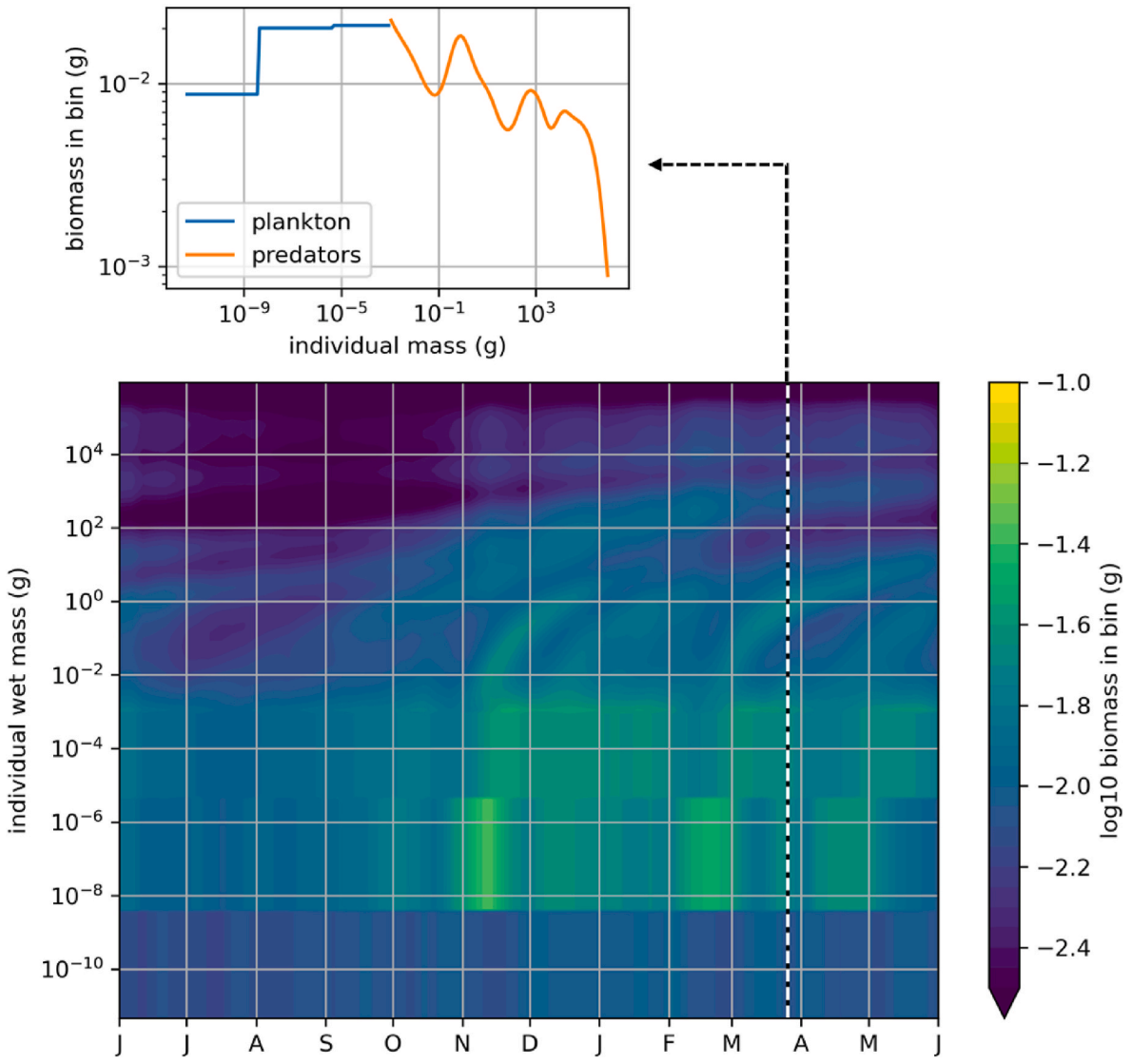

Fig. 5. The modelled size spectrum (4.2 pg–1000 kg) for the period preceding low catch per unit effort for *L. reynaudii* (1 June 2012–31 May 2013), bottom panel, along with a snapshot for a single day (March 26, 2013), top panel. Both plots show the biomass per bin (expected slope = 0, Sheldon et al., 1972) instead of the biomass density (expected slope = −1) in order to highlight variability. In the bottom panel, the x axis denotes time, indicated with the initial letter of each month. In the snapshot, the blue line shows the plankton biomass taken from MEDUSA (non-diatoms, diatoms + microzooplankton, mesozooplankton), the orange line shows the biomass in the 100 size classes of the community size spectrum model. The y axis of the bottom spectrum matches the x axis of the snapshot.

the Environment (DFFE). The catch per unit effort (CPUE) is defined as total catch (kg) per man hour fished (Roel, 1998). For each calendar year, values are reported separately for Jan–Mar and Apr–Dec. However, as shown in Fig. 3, the peak in catches generally falls in Dec–Jan. These two months are part of the same late spring-early summer spawning season but belong to different reporting intervals. As a metric for annual CPUE, we combine these intervals in an Apr–Mar average (Fig. 4), which encompasses a single spawning season and thus the output of a single generation of squid. Other studies have used CPUE or catch averaged over a *calendar* year (Jan–Dec), but as this metric combines the output of two non-overlapping generations of squid, it is likely not easily explained in terms of a single, biologically plausible annual driver. The validity of combining Mar–Dec and the subsequent Jan–Mar is demonstrated by the fact that CPUE values in Jan–Mar are generally more similar to CPUE in Apr–Dec the year before ($r = 0.70$) than Apr–Dec of the same year ($r = 0.47$). In the remainder of this work, we will attempt to explain the interannual variability in CPUE, shown in Fig. 4, in terms of the variability in the size spectrum model introduced in the previous section.

2.3.2. *Correlation analysis*

The outputs of the community size spectrum model – time series of total predator biomass (g/m^2) in 100 size classes between 1 mg and 1000 kg – are treated as potential predictors of CPUE of *L. reynaudii*. As we focus exclusively on the pelagic paralarval stage, we narrow this down to size classes with individual mass below 100 g, and the 150 d period between 2 December – 31 May which should include the paralarval stage of individuals produced as part of the Sep–Dec spawning season.

We use Spearman rank correlation (as opposed to Pearson correlation) to quantify the relationship between candidate predictors and catch. This metric is designed to identify relationships that are monotonic, but not necessarily linear. That is ideal for our purpose as any monotonic relationship (linear, saturating, exponential, etc.) would be helpful to predict catch.

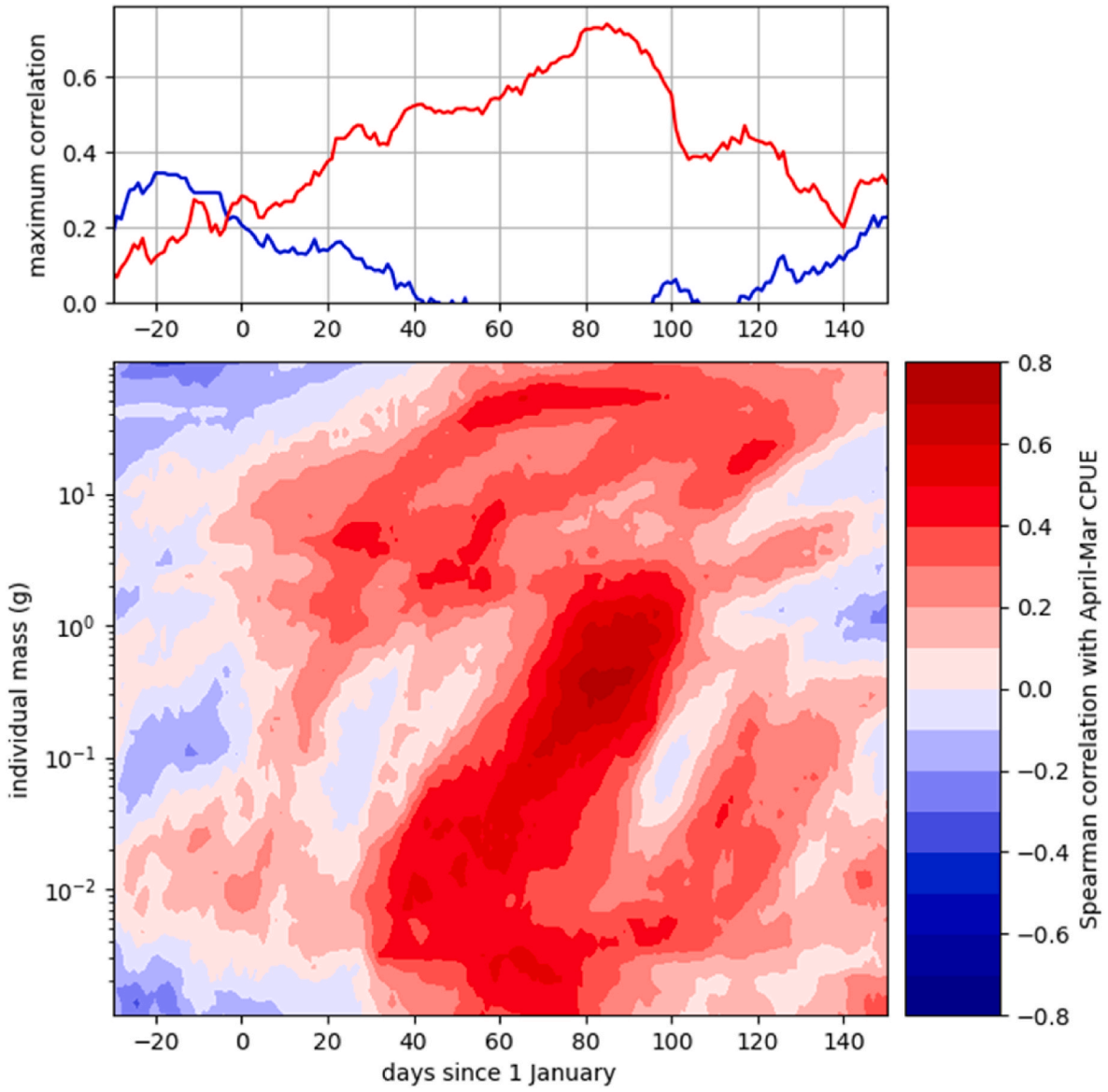

Fig. 6. Correlation between *L. reynaudii* catch per unit effort and biomass in single class of the size spectrum model, as a function of size class and season. This is based on correlation coefficients computed on a grid of 56 size classes (1 mg–100 g, y-axis) and 150 times (−30 to 120 d since 1 January, daily resolution, x-axis). The top panel shows the maximum positive (red) and negative (blue) correlation across the size spectrum (y axis of the bottom panel – note that this axis shows the absolute value of the correlation coefficient and thus only takes non-negative values).

Table 1
Timing of life history transitions of the squid *L. reynaudii*, inferred by a Dynamic Energy Budget model. All values are percentiles over an ensemble of 500,000 parameter sets drawn from the posterior distribution. Food availability (the value for the functional response) was set to 0.6 (Hartvig et al., 2011) and the ambient temperature to 17.3°C. Ages refer to the time since fertilization; durations to the time since hatching.

Life history statistic	Median (95% conf. int.)	Figure
Age at hatching (duration of egg development)	26 d (24–28 d)	A4.a
Age at start of feeding	30 d (28–32 d)	
Age at end of paralarval stage	103 d (88–123 d)	A4.c
Age at maturity	296 d (157–482 d)	A4.d
Duration of non-feeding stage	3.8 d (2.6–5.0 d)	A4.b
Duration of paralarval stage	76 d (62–96 d)	8b
Wet mass at end of paralarval stage	0.74 g (0.35–1.60 g)	8c

3. Results

3.1. Community size spectrum

The 1995–2015 average of the slope of the modelled biomass density spectrum is −1.03 (range: −1.05 to −1.02) though this differs slightly between the plankton (−0.99 to −0.90) and the predator communities (−1.12 to −1.05). These values are close to the slope of −1 expected for a classic Sheldon-Sutcliffe spectrum (Sheldon et al., 1972). The seasonal variability of the spectrum becomes apparent when we plot the biomass per bin (expected slope 0), as done for the period 1 June 2012–31 May 2013 in Fig. 5. This shows plankton blooms in November and February that propagate as waves through the predator spectrum, being delayed and dampened as they progress upward (in mass) and rightward (in time) through the size spectrum. These waves fade out around a biomass of 100 g. The biomass of large individuals is less variable in time.

3.2. Correlation between predicted biomass and catch

Fig. 6 shows the Spearman rank correlation between observed CPUE and modelled biomass in the smaller size classes (1 mg–100 g, y axis) for the period of December till May (x axis). The correlation coefficient reaches a maximum of 0.74 on day 85 and an individual mass of 0.37 g. This point is surrounded by a larger region with high (>0.5) correlation coefficients which can be seen to start from the lower left (earlier in time, lower biomass), e.g., 0.003 g around day 40, 0.03 g on day 60. The upward (increase in mass) and rightward (increase in time) trends in correlation contours is the result of growth of individuals over time.

Fig. 7 shows the CPUE prediction obtained for the highest correlation coefficient. For each year, it shows CPUE (y-axis) plotted against the modelled biomass in individuals with a mass of 0.37 g on day 85 (x-axis).

3.3. Simulated growth and life history of squid

Fig. 8 shows the ensemble of growth curves of *L. reynaudii* simulated with 500,000 realisations of the bioenergetic model. Corresponding statistics per parameter are given in Table A.1. Wet mass is well constrained throughout the simulation, not just during early development where observations are available (Fig. A.2). The increase in wet mass during the first 80–90 days is approximately exponential (linear in Fig. 8a, which uses a log-transformed y-axis); after that, growth slows down.

The bioenergetic model makes explicit predictions about stage durations and the timing of life history events. These predictions are summarized in Table 1. The probability distribution of the duration of the paralarval stage and its final wet mass are shown in more detail in the inset panel of Fig. 8. In short, the paralarval stage is expected to last 76 d (62–96 d), which means it would end 103 d (95% C.I. 88–122 d) after fertilization. At this time *L. reynaudii* wet mass is expected be 0.74 g (0.35–1.60 g). Probability distributions for duration of egg development, duration of the non-feeding stage, age at the end of the paralarval stage, and age at maturity are shown in Fig. A.4. Physiological rates in the bioenergetic model are temperature-dependent; consequently, predicted timings of life history events are too. As the model captures the observed temperature dependence of egg development (Fig. A.1), its temperature response appears to be appropriate for at least the early life stages of *L. reynaudii*, and thus, suitable for predicting the timing of associated life history transitions.

4. Discussion

4.1. An ecologically plausible predictor of CPUE?

The highest correlation between 1995 and 2015 CPUE and the modelled size spectrum over the Agulhas Bank is found on day 85 of the year (26–27 Mar): that day shows a correlation of 0.74 between observed CPUE and the simulated density (g/m^2) of individuals of 0.37 g. Does this size and timing relate in a meaningful way to the life cycle of *Loligo reynaudii*? The bioenergetic model predicts that a *L. reynaudii* individual of 0.37 g has hatched 68 days ago (95% confidence interval: 62–78 d) from eggs that were deposited 95 days ago (95% CI: 87–105 d) (Fig. 8). Thus, the hatching peak that produced 0.37 g individuals on day 85 would be centred on 17 Jan, and the associated spawning peak on 21 Dec. As correlations are based on a 90-day running mean of size spectrum predictions, this broadens to 90-day long hypothetical spawning and hatching periods: 6 Nov – 4 Feb and 3 Dec – 2/3 Mar respectively. Results could suggest that the fate of paralarvae produced during this period ultimately explains 55% of the variability in CPUE. This timeline is summarized in Fig. 9.

At first glance, this correlation is ecologically plausible: the hypothetical timing of the spawning that underpins the correlation (6 Nov – 4 Feb) overlaps with the Sep–Dec spawning season (Augustyn et al., 1994; Melo and Sauer, 1998) that can be expected to produce the bulk of all paralarvae. Yet this overlap is only partial: spawning starts two months earlier in reality. Why would a predictor for CPUE not account for this early spawning? It is important to realise that our annual CPUE metric (total annual catch/total annual effort) is biased towards periods of high catch, notably Dec and Jan, which together make up over one third of annual catch (Fig. 3). Thus, the best predictor for CPUE will naturally emphasise the role of processes (e.g., spawning episodes) that contribute to the Dec–Jan stock. As the *L. reynaudii* life cycle is approximately annual (one year between fertilization and peak reproduction), the individuals that make up Dec–Jan stock may be expected to have been produced during spawning that happens close to 12 months earlier, i.e., precisely the period around the end of December pointed to by our CPUE predictor. This does not yet explain why the reported Sep–Dec spawning is not clearly reflected in catch statistics (Fig. 3). Likely, this is due in part to the annual closures that the *L. reynaudii* fishery is subjected. These typically include the last week of Oct until mid Nov (Cochrane et al., 2014; Roel et al., 1998).

The above suggests that our CPUE correlation arises because the size spectrum model captures the conditions (food availability and predation pressure) during the first 68 days of *L. reynaudii* development. Accordingly, Fig. 6 shows that, over this period, the model's predictive skill (the correlation coefficient) gradually increases in time (x-axis) and individual size (y-axis). However, this begs the question of why the correlation peaks at day 85 and does not continue to increase. To answer this, it is insightful to note that this peak occurs for individuals of 0.37 g: approximately the minimum wet mass of *L. reynaudii* at the end of its paralarval stage (95% CI: 0.35–1.60 g; Table 1, Fig. 8c). As our modelling is exclusively focused on the pelagic environment, it is not expected to have predictive power after the onset of diel vertical migration and part-demersal feeding that defines the end of the paralarval stage (Shea and Vecchione, 2010; Young and Harman, 1988). Thus, a natural upper mass limit on the model's predictive power would lie between 0.35 and 1.60 g in the size spectrum. It is encouraging that this threshold emerges

in Fig. 6. The fact that the maximum correlation is found at the maximum wet mass expected for paralarvae suggests that it is food availability and predation pressure over the entire 76-day long paralarval phase (Table 1), not just the first few days, that determines the next spawning stock (cf. Roberts, 2005).

4.2. Possible mechanisms

What mechanisms ultimately explain the interannual variability in the modelled number of individuals emerging from the paralarval stage? To answer this, it is particularly informative to review what phenomena the models *cannot* (faithfully) represent. First of these is the production of the eggs that produce the paralarvae. The size spectrum model does not include a stock-recruitment relationship: production of the smallest size class of predators is determined only by the availability of their plankton prey, not by the presence of larger-sized, reproducing individuals. While the absence of a a stock-recruitment relationship is a common feature of models that represent the entire community of predator species with a single size spectrum (Blanchard et al., 2009; Woodworth-Jefcoats et al., 2013), it implies that variation in spawning stock cannot influence the next generation of juveniles. When we interpret model results in terms of *L. reynaudii* abundance, we thus effectively assume that egg production each year is sufficient to obscure any relationship between spawning stock and paralarval recruitment. This is supported by the fact that stock-recruitment relationships are not usually observed in cephalopods; environmental variability, particularly during early life stages, is expected to underlie variability in stock size (Pierce et al., 2008).

Next, the model only includes a limited representation of environmental variability and its impact on paralarvae. For example, the size spectrum model we use for higher trophic levels, including *L. reynaudii,* is horizontally averaged. Thus it cannot account for spatial patterns over the Agulhas Bank, e.g., mismatches between *L. reynaudii* and its prey, nor can it account for local currents. Therefore, transport of newly hatched larvae to nursing grounds, as proposed by the "Western Transport Hypothesis" (Martins et al., 2014; Roberts, 2005), cannot contribute to our explanation for 55% of CPUE variability. Moreover, the size spectrum model does not consider transport of *L. reynaudii* over the boundaries of the Agulhas Bank domain. Thus, loss of paralarvae due to off-shelf advection (Downey-Breedt et al., 2016; Roberts et al., 2012; Roberts and van den Berg, 2002; Jacobs et al. under rev) cannot feature as part of the explanation.

To better understand the interannual skill of our predictor, it is worth revisiting the representation of temporal variability in the model and, in particular, its sources of interannual variability. The size spectrum model uses a relatively simple set of rules to extend the plankton spectrum to higher trophic levels. All calendar-date specific forcing is taken from NEMO-MEDUSA. While this, in turn, is a highly detailed model in many respects, notably spatially, its calendar-date-specific inputs are limited to meteorological conditions taken from reanalysis (Brodeau et al., 2010; Dussin et al., 2016). This implies that any realistic patterns in modelled interannual variability must ultimately originate from meteorology. What is more, only some of the processes described by NEMO-MEDUSA depend *in pronounced, predictable ways* on meteorological conditions. For instance, the timing of wind-driven upwelling and its impact on primary production can be captured correctly, whereas mesoscale variability, e.g., meanders in the Agulhas current, cannot be accurately captured due to its intrinsically chaotic nature (Jacobs et al., 2020, 2022; Robinson et al., 2016; Srokosz et al., 2015). We hypothesise that weather-driven interannual variability in upwelling over the Agulhas Bank (Jebri et al., 2022) leads to predictable changes in the size structure of the plankton community (total biomass and/or the ratio of small to large plankton types). These changes then lead to a response in the size spectrum of higher trophic levels, notably the 1 mg–1 g wet mass range that the size spectrum model reliably reproduces. At that point, it may come down to the smallest predators, e.g., paralarvae, trying to catch a wave in the plankton spectrum that is just not present every single year (Pope et al., 1994).

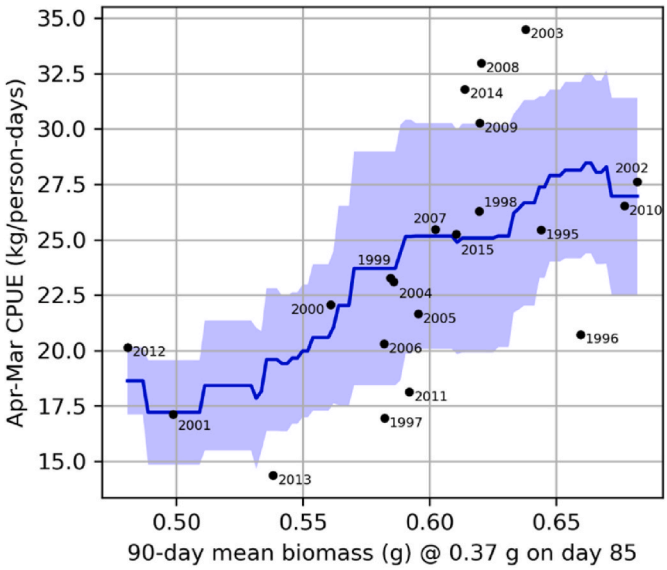

Fig. 7. Correlation plot for the best predictor of *L. reynaudii* catch (maximum correlation in Fig 6), showing catch per unit effort for individual years (each value repesentative for April till March the following year) as a function of modelled biomass in the best predicting size class (0.37 g). The line shows the running mean with a window size of 0.15 g; the shaded area shows the corresponding running standard deviation.

It is worth emphasising that the above discussion on potential mechanisms is specifically about the best predictor we have identified (biomass in individuals of 0.37 g on day 85). This predictor explains 55% of the variability. While this is promising, it also leaves 45% of variability *un*explained. Thus, other mechanisms that have previously been proposed to explain interannual variability in *L. reynaudii* catch, e.g., the influence of temperature and turbidity on spawning (Roberts and Sauer, 1994) and of currents on early life stages (Roberts, 2005), may still have a role to play. As several of these variables are primarily wind-driven, they can potentially be faithfully described by models such as NEMO-MEDUSA. It is therefore conceivable to ultimately combine our size-spectrum-based predictor with these variables in a multivariate predictor with greater skill.

4.3. Life history of L. reynaudii

While the bioenergetic model makes wide-ranging predictions about the growth, reproduction, and survival of *L. reynaudii* (Fig. A.3), our interpretation of the CPUE correlation depends exclusively on the predicted growth curve and the duration of the paralarval phase (Fig. 8). These model features are robust; they are constrained by experimental observations of egg development (Oosthuizen et al., 2002) and paralarval growth (Vidal et al., 2005). Perhaps the most central prediction is that the duration of the paralarval phase (i.e., the initial exponential growth phase) is 76 d at 17.3 °C (Fig. 8b; Table 1). This metric indicates the time spent as planktonic larva in the pelagic and has important implications, for example, Lagrangian modelling studies (Downey-Breedt et al., 2016; Martins et al., 2014; Jacobs et al. under rev). Our predicted value agrees closely with the two to three months reported for *L. vulgaris* (González et al., 2010; Mangold-Wirz, 1963). It also differs markedly from the value of 40 d adopted by earlier modelling studies (Downey-Breedt et al., 2016; Martins et al., 2014). However, their value was based on experiments with *Doryteuthis opalescens*. While this species does have a paralarval phase lasting 35–45 d (Vidal et al., 2018), its lifespan is markedly shorter than that of *L. reynaudii* (6–9 months vs. 15–18 months) (Butler et al., 1999). The duration of its paralarval stage

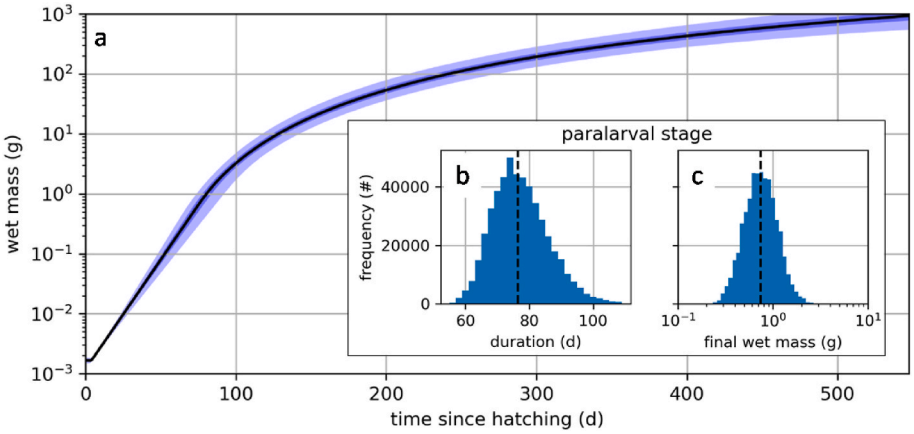

Fig. 8. Growth of the squid *L. reynaudii* in its first 18 months, predicted by a Dynamic Energy Budget model. Results are based on simulations with an ensemble of 500,000 parameter sets drawn from the posterior distribution. Solid lines show the median result; shaded areas show the 2.5–97.5% (light) and 25–75% (dark) confidence intervals. Food availability is represented by a value for the functional response of 0.6 (Hartvig et al., 2011); the ambient temperature is set to 17.3°C. Inset panels show histograms of the estimated (b) duration of the of the paralarval stage and (c) wet mass at the end of the paralarval stage. For exact values, see Table 1.

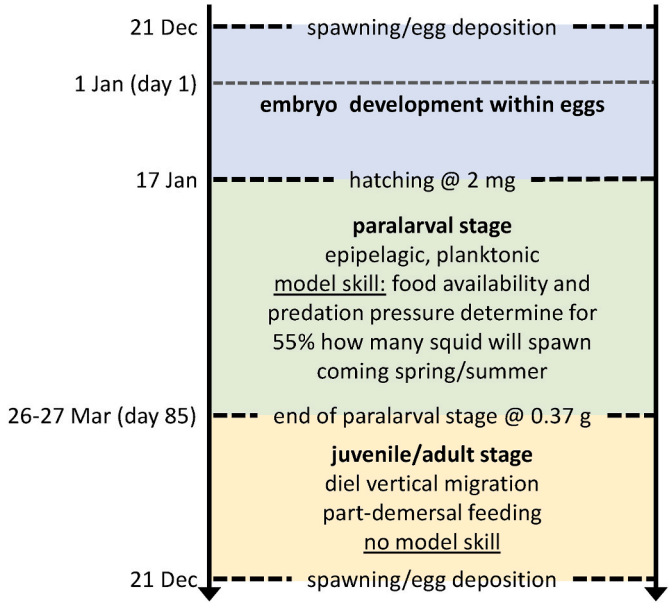

Fig. 9. Proposed timeline for *L. reynaudii* life history. This timeline combines results of the size spectrum and bioenergetic models to explain the emergence of a maximum correlation between predicted abundance of individuals of 0.37 g at day 85 of the year and catch per unit effort over the subsequent period (primarily Dec-Jan). All numbers are subject to uncertainty; confidence intervals are given in the main text and Table 1.

is therefore likely less than that of *L. reynaudii*.

The bioenergetic model presented here could potentially describe the entire life history of *L. reynaudii* in the field, from fertilization to maturity, reproduction and death. The model already describes these features (Fig. A.3), although it would benefit from additional observations on reproduction rate and longevity to further constrain reproductive output and survival. Several further advances would be required to describe the complete life cycle of squid in the field, however. First, it would require explicit representation of the temporal variation in food availability and predation pressure within the bioenergetic model. This could be achieved by dynamically coupling it to the size spectrum model, though we note such coupling is non-trivial to implement and, in all likelihood, considerably more computationally costly to run. Thus, detailed exploration of model uncertainty, achieved here with an ensemble of 500,000 parameterisations, may no longer be possible. Moreover, use of such a coupled model beyond the paralarval stage would require a more detailed representation of the vertical structure of the community represented by the size spectrum, and of the vertical positioning of *L. reynaudii* after it starts diel vertical migration and demersal feeding. Such developments are feasible (Petrik et al., 2019; van Denderen et al., 2021) but they would unavoidably produce models that are more complex and dependent on numerous additional assumptions. Still, the use of coupled models also has advantages as it would allow for explicit representation of the differences between squid and the fish that make up most of the background community, for instance, in growth rate (squid grow faster than fish) and prey selectivity (squid take a wider range of prey sizes).

4.4. Predicting catch of cephalopods

There is a long history of modelling relationships between environment and squid catch for the purpose of prediction or forecasting (Moustahfid et al., 2021; Rodhouse et al., 2014). In most of this work, however, the emphasis lies on empirical statistical relationships between stock size (or CPUE) and environmental variables, e.g., temperature (Roberts, 2005; Waluda et al., 2001) or chlorophyll (Jebri et al., 2022). The use of process-based models is less common and often takes the form of highly complex end-to-end ecosystem models such as Ecopath with Ecosim (Gasalla et al., 2010) or Atlantis (Jackson et al., 2007); a comprehensive overview is given by de la Chesnais et al. (2019). In contrast to these approaches, our core model is a parameter-sparse, non-spatial, size-based ecosystem model (Blanchard et al., 2009; Cheung et al., 2018), revolving around trophic interactions and their impact on food availability and predation pressure. This makes it different from most other approaches (Rodhouse et al., 2014).

There is at least a seven-month delay between our predictor with highest correlation (biomass in individuals of 0.37 g between 7 Feb and 8/9 May) and the peak in catches (Dec). It therefore has the potential to serve as an early warning indicator of bad catch periods. For instance, a simple threshold could be used to classify model predictions into good catch and bad catch years (e.g., by separating at x = 0.6 in Fig. 7). Such an early warning system would not need to be model-based. For example, our results indicate that valuable information may be gleaned from paralarval abundance, and more specifically, their size distribution. This could be determined through repeated field surveys, e.g., in Feb, Mar, Apr, as our predictor performs best when based on 90 day

means of biomass.

Alternatively, the size spectrum model presented here could be run operationally to deliver near-real time projections for the state of the Agulhas Bank ecosystem. The main challenge for such an approach is to source the data to drive this model: depth-resolved temperature and biomasses of different size classes of plankton over the Agulhas Bank. These variables could come from a coupled hydrodynamic-biogeochemical model such as NEMO-MEDUSA, but no model with sufficiently high spatial resolution and sufficient detail in its representation of the plankton community is currently run operationally for the Agulhas region. Instead, we can attempt to quantify the variables driving the size spectrum model through remote sensing (Appendix B), but this presents multiple challenges due to the need for depth-resolved information about the structure of the plankton community. These challenges may be overcome in the future thanks to the development of new satellite products and sensors such as hyperspectral ocean-colour sensors that provide further insight into plankton community structure (Cael et al., 2020) and Lidar-based observation of zooplankton (Behrenfeld et al., 2019). Overall, the greatest promise is held by further integration of in-situ observations, remote sensing observations and operational models (Brewin et al., 2021), for instance, the use of operational hydrodynamic-biogeochemical models with Plankton Functional Type based data assimilation (Skákala et al., 2018).

5. Conclusions

We find a correlation of 0.74 between annual *Loligo reynaudii* catch per unit effort (CPUE) and modelled abundance of pelagic organisms of 0.37 g at the end of March over a 21-year period (1995–2015). *L. reynaudii* individuals of this size are estimated to be near the end of their paralarval stage and to have hatched from eggs deposited 103 days earlier. This suggests that the fate of paralarvae produced from Dec spawning can explain 55% of the interannual variability in next year's CPUE. As CPUE is weighted towards the time of peak catch – Dec–Jan – the pattern we found suggests that: (1) the life cycle *L. reynaudii* is predominantly annual, with 12 months between fertilization and peak reproduction, and (2) the bottleneck for the population is the paralarval stage (mid Jan-end Mar), with food availability and predation pressure during this period being the principal factor that determines spawning stock biomass and CPUE the following spring/summer. Our results imply that over half the variability in CPUE can be predicted from the model's main drivers: the size structure and depth distribution of the phytoplankton and zooplankton community. As these properties are not easily observed over large areas, catch predictions would benefit from the development of operational hydrodynamic-biogeochemical models covering the Agulhas Bank.

Author statement

J.B. designed and implemented the methodology, performed all analyses, and wrote the manuscript with input from all authors.

Declaration of competing interest

The authors declare that they have no known competing financial interests or personal relationships that could have appeared to influence the work reported in this paper.

Acknowledgements

The study was supported by the Global Challenges Research Fund (GCRF) under NERC grant NE/P021050/1 in the framework of the SOLSTICE-WIO project (https://www.solstice-wio.org). This work is also part of the UK-SA Bilateral Chair in Ocean Science and Marine Food Security funded by the British Council Newton Fund grant SARCI 1503261 16102/NRF98399. Robert Brewin was supported by a UKRI Future Leader Fellowship (MR/V022792/1). The authors thank Dr Jean Githaiga from the South African Department of Forestry, Fisheries and the Environment for providing updated CPUE data. The description and presentation of this work greatly benefited from comments and suggestions made by two anonymous reviewers.

Appendix A. Supplementary data

Supplementary data to this article can be found online at https://doi.org/10.1016/j.dsr2.2022.105123.

References

Arkhipkin, A.I., Roa-Ureta, R., 2005. Identification of ontogenetic growth models for squid. Mar. Freshw. Res. 56, 371. https://doi.org/10.1071/MF04274.

Augustyn, C.J., 1990. Biological studies on the chokker squid *Loligo vulgaris reynaudii* (Cephalopoda; Myopsida) on spawning grounds off the south-east coast of South Africa. S. Afr. J. Mar. Sci. 9, 11–26. https://doi.org/10.2989/025776190784378736.

Augustyn, C.J., Lipiński, M.R., Sauer, W.H.H., 1992. Can the Loligo squid fishery be managed effectively? A synthesis of research on *Loligo vulgaris reynaudii*. S. Afr. J. Mar. Sci. 12, 903–918. https://doi.org/10.2989/02577619209504751.

Augustyn, C.J., Lipiński, M.R., Sauer, W.H.H., Roberts, M.J., Mitchell-Innes, B.A., 1994. Chokka squid on the Agulhas Bank: life history and ecology. South Afr. J. Sci. 90, 143–154.

Augustyn, C.J., Roel, B.A., 1998. Fisheries biology, stock assessment, and management of the chokka squid (*Loligo vulgaris reynaudii*) in South African waters: an overview. Calif. Coop. Ocean. Fish. Investig. Rep. 39, 71–80.

Behrenfeld, M.J., Gaube, P., Della Penna, A., O'Malley, R.T., Burt, W.J., Hu, Y., Bontempi, P.S., Steinberg, D.K., Boss, E.S., Siegel, D.A., Hostetler, C.A., Tortell, P.D., Doney, S.C., 2019. Global satellite-observed daily vertical migrations of ocean animals. Nature 576, 257–261. https://doi.org/10.1038/s41586-019-1796-9.

Blanchard, J.L., Andersen, K.H., Scott, F., Hintzen, N.T., Piet, G., Jennings, S., 2014. Evaluating targets and trade-offs among fisheries and conservation objectives using a multispecies size spectrum model. J. Appl. Ecol. 51, 612–622. https://doi.org/10.1111/1365-2664.12238.

Blanchard, J.L., Jennings, S., Holmes, R., Harle, J., Merino, G., Allen, J.I., Holt, J., Dulvy, N.K., Barange, M., 2012. Potential consequences of climate change for primary production and fish production in large marine ecosystems. Phil. Trans. Biol. Sci. 367, 2979–2989. https://doi.org/10.1098/rstb.2012.0231.

Blanchard, J.L., Jennings, S., Law, R., Castle, M.D., McCloghrie, P., Rochet, M.-J., Benoît, E., 2009. How does abundance scale with body size in coupled size-structured food webs? J. Anim. Ecol. 78, 270–280. https://doi.org/10.1111/j.1365-2656.2008.01466.x.

Boudreau, P.R., Dickie, L.M., 1992. Biomass spectra of aquatic ecosystems in relation to fisheries yield. Can. J. Fish. Aquat. Sci. 49, 1528–1538. https://doi.org/10.1139/f92-169.

Boyle, P., Rodhouse, P., 2005. Cephalopods: Ecology and Fisheries. Wiley-Blackwell. https://doi.org/10.1002/9780470995310.

Brewin, R.J.W., Sathyendranath, S., Platt, T., Bouman, H., Ciavatta, S., Dall'Olmo, G., Dingle, J., Groom, S., Jönsson, B., Kostadinov, T.S., Kulk, G., Laine, M., Martínez-Vicente, V., Psarra, S., Raitsos, D.E., Richardson, K., Rio, M.-H., Rousseaux, C.S., Salisbury, J., Shutler, J.D., Walker, P., 2021. Sensing the ocean biological carbon pump from space: a review of capabilities, concepts, research gaps and future developments. Earth Sci. Rev. 217, 103604 https://doi.org/10.1016/j.earscirev.2021.103604.

Brodeau, L., Barnier, B., Treguier, A.M., Penduff, T., Gulev, S., 2010. An ERA40-based atmospheric forcing for global ocean circulation models. Ocean Model. 31, 88–104. https://doi.org/10.1016/j.ocemod.2009.10.005.

Bruggeman, J., Heringa, J., Brandt, B.W., 2009. PhyloPars: estimation of missing parameter values using phylogeny. Nucleic Acids Res. 37, W179–W184. https://doi.org/10.1093/nar/gkp370.

Butler, J., Fuller, D., Yaremko, M., 1999. Age and growth of market squid (*Loligo opalescens*) off California during 1998. Calif. Coop. Ocean. Fish. Investig. Rep. 40, 191–195.

Cael, B.B., Chase, A., Boss, E., 2020. Information content of absorption spectra and implications for ocean color inversion. Appl. Opt. 59, 3971. https://doi.org/10.1364/AO.389189.

Cheung, W.W.L., Bruggeman, J., Butenschön, M., 2018. Projected changes in global and national potential marine fisheries catch under climate change scenarios in the twenty-first century. In: Barange, M., Bahri, T., Beveridge, M.C.M., Cochrane, K.L., Funge-Smith, S., Poulain, F. (Eds.), Impacts of Climate Change on Fisheries and Aquaculture: Synthesis of Current Knowledge, Adaptation and Mitigation Options. FAO Fisheries Technical Paper 627. FAO, Rome.

Cochrane, K.L., Oliver, B., Sauer, W., 2014. An assessment of the current status of the chokka squid fishery in South Africa and an evaluation of alternative allocation strategies. Mar. Pol. 43, 149–163. https://doi.org/10.1016/j.marpol.2013.05.006.

Datta, S., Blanchard, J.L., 2016. The effects of seasonal processes on size spectrum dynamics. Can. J. Fish. Aquat. Sci. 73, 598–610. https://doi.org/10.1139/cjfas-2015-0468.

de la Chesnais, T., Fulton, E.A., Tracey, S.R., Pecl, G.T., 2019. The ecological role of cephalopods and their representation in ecosystem models. Rev. Fish Biol. Fish. 29, 313–334. https://doi.org/10.1007/s11160-019-09554-2.

Downey-Breedt, N.J., Roberts, M.J., Sauer, W.H.H., Chang, N., 2016. Modelling transport of inshore and deep-spawned chokka squid (*Loligo reynaudi*) paralarvae off South Africa: the potential contribution of deep spawning to recruitment. Fish. Oceanogr. 25, 28–43. https://doi.org/10.1111/fog.12132.

Dussin, R., Barnier, B., Brodeau, L., Molines, J.M., 2016. The Making of Drakkar Forcing Set DFS5, DRAKKAR/MyOcean Report 01-04-16. Laboratoire de Glaciologie et Géophysique de l'Environnement, Grenoble, France.

Evans, G.T., Parslow, J.S., 1985. A model of annual plankton cycles. Biol. Oceanogr. 3, 327–347. https://doi.org/10.1080/01965581.1985.10749478.

Forsythe, J.W., van Heukelem, W.F., 1987. Growth. In: Boyle, P.R. (Ed.), Cephalopod Life Cycles. 2. Comparative Reviews. Academic Press, London, pp. 135–156.

Gasalla, M.A., Rodrigues, A.R., Postuma, F.A., 2010. The trophic role of the squid *Loligo plei* as a keystone species in the South Brazil Bight ecosystem. ICES (Int. Counc. Explor. Sea) J. Mar. Sci. 67, 1413–1424. https://doi.org/10.1093/icesjms/fsq106.

GEBCO Compilation Group, 2020. GEBCO 2020 Grid. https://doi.org/10.5285/a29c5465-b138-234d-e053-6c86abc040b9.

González, Á.F., Otero, J., Pierce, G.J., Guerra, Á., 2010. Age, growth, and mortality of *Loligo vulgaris* wild paralarvae: implications for understanding of the life cycle and longevity. ICES (Int. Counc. Explor. Sea) J. Mar. Sci. 67, 1119–1127. https://doi.org/10.1093/icesjms/fsq014.

Grist, E.P.M., Jackson, G.D., 2004. Energy balance as a determinant of two-phase growth in cephalopods. Mar. Freshw. Res. 55, 395. https://doi.org/10.1071/MF03154.

Haario, H., Saksman, E., Tamminen, J., 2001. An adaptive metropolis algorithm. Bernoulli 7, 223–242. https://doi.org/10.2307/3318737.

Hartvig, M., Andersen, K.H., Beyer, J.E., 2011. Food web framework for size-structured populations. J. Theor. Biol. 272, 113–122. https://doi.org/10.1016/j.jtbi.2010.12.006.

Hunsicker, M.E., Essington, T.E., Watson, R., Sumaila, U.R., 2010. The contribution of cephalopods to global marine fisheries: can we have our squid and eat them too? Fish Fish. 11 (4), 421–438. https://doi.org/10.1111/j.1467-2979.2010.00369.x.

Jackson, G.D., Bustamante, P., Cherel, Y., Fulton, E.A., Grist, E.P.M., Jackson, C.H., Nichols, P.D., Pethybridge, H., Phillips, K., Ward, R.D., Xavier, J.C., 2007. Applying new tools to cephalopod trophic dynamics and ecology: perspectives from the Southern Ocean Cephalopod Workshop, February 2–3, 2006. Rev. Fish Biol. Fish. 17, 79–99. https://doi.org/10.1007/s11160-007-9055-9.

Jacobs, Z., Roberts, M., Jebri, F., Srokosz, M., Kelly, S., Sauer, W., Bruggeman, J., Popova, E., 2022. Drivers of productivity on the Agulhas Bank and the importance for marine ecosystems. Deep Sea Res. Part II Top. Stud. Oceanogr. 199, 105080 https://doi.org/10.1016/j.dsr2.2022.105080.

Jackson, G.D., O'Dor, R.K., 2001. Time, space and the ecophysiology of squid growth, life in the fast lane. Vie Milieu 51, 205–215.

Jacobs, Z.L., Jebri, F., Raitsos, D.E., Popova, E., Srokosz, M., Painter, S.C., Nencioli, F., Roberts, M., Kamau, J., Palmer, M., Wihsgott, J., 2020. Shelf-break upwelling and productivity over the North Kenya banks: the importance of large-scale ocean dynamics. J. Geophys. Res.: Oceans 125, 1–18. https://doi.org/10.1029/2019JC015519.

Jebri, F., Raitsos, D.E., Gittings, J.A., Jacobs, Z.L., Srokosz, M., Gornall, J., Sauer, W.H.H., Roberts, M.J., Popova, E., 2022. Unravelling links between squid catch variations and biophysical mechanisms in South African waters. Deep Sea Res. Part II Top. Stud. Oceanogr. 196, 105028 https://doi.org/10.1016/j.dsr2.2022.105028.

Jennings, S., Warr, K., Mackinson, S., 2002. Use of size-based production and stable isotope analyses to predict trophic transfer efficiencies and predator-prey body mass ratios in food webs. Mar. Ecol. Prog. Ser. 240, 11–20. https://doi.org/10.3354/meps240011.

Kooijman, S.A.L.M., 2014. Metabolic acceleration in animal ontogeny: an evolutionary perspective. J. Sea Res. 94, 128–137. https://doi.org/10.1016/j.seares.2014.06.005.

Kooijman, S.A.L.M., 2010. Dynamic Energy Budget Theory for Metabolic Organisation, third ed. Cambridge University Press, Cambridge, UK. https://doi.org/10.1017/CBO9780511805400.

Lipiński, M., van der Vyver, J., Shaw, P., Sauer, W., 2016. Life cycle of chokka-squid *Loligo reynaudii* in South African waters. Afr. J. Mar. Sci. 38, 589–593. https://doi.org/10.2989/1814232X.2016.1230074.

Lipiński, M.R., 2002. Growth of cephalopods: conceptual model. Gabhanlungen der Geologischen Bundesanstalt 57, 133–138.

Lipiński, M.R., 1992. Cephalopods and the Benguela ecosystem: trophic relationships and impact. S. Afr. J. Mar. Sci. 12, 791–802. https://doi.org/10.2989/02577619209504742.

Lipiński, M.R., 1987. Food and feeding of *Loligo vulgaris reynaudii* from St Francis Bay, South Africa. S. Afr. J. Mar. Sci. 5, 557–564. https://doi.org/10.2989/025776187784522513.

Macewicz, B.J., Hunter, J.R., Lo, N.C.H., LaCasella, E.L., 2004. Fecundity, egg deposition, and mortality of market squid (*Loligo opalescens*). Fish. Bull. 102, 306–327.

Mangold-Wirz, K., 1963. Biologie des céphalopodes benthiques et nectoniques de la Mer Catalane. Vie Milieu: bulletin du Laboratoire Arago. Supplément no 13.

Marques, G.M., Augustine, S., Lika, K., Pecquerie, L., Domingos, T., Kooijman, S.A.L.M., 2018. The AmP project: comparing species on the basis of dynamic energy budget parameters. PLoS Comput. Biol. 14, e1006100 https://doi.org/10.1371/journal.pcbi.1006100.

Martins, R.S., Roberts, M.J., Lett, C., Chang, N., Moloney, C.L., Camargo, M.G., Vidal, E. A.G., 2014. Modelling transport of chokka squid (*Loligo reynaudii*) paralarvae off South Africa: reviewing, testing and extending the "Westward Transport Hypothesis. Fish. Oceanogr. 23, 116–131. https://doi.org/10.1111/fog.12046.

Martins, R.S., Roberts, M.J., Vidal, É.A.G., Moloney, C.L., 2010. Effects of temperature on yolk utilization by chokka squid (*Loligo reynaudii* d'Orbigny, 1839) paralarvae. J. Exp. Mar. Biol. Ecol. 386, 19–26. https://doi.org/10.1016/j.jembe.2010.02.014.

Melo, Y., Sauer, W.H.H., 2007. Determining the daily spawning cycle of the chokka squid, *Loligo reynaudii* off the South African Coast. Rev. Fish Biol. Fish. 17, 247–257. https://doi.org/10.1007/s11160-006-9034-6.

Melo, Y.C., Sauer, W.H.H., 1998. Ovarian atresia in cephalopods. S. Afr. J. Mar. Sci. 20, 143–151. https://doi.org/10.2989/025776198784126539.

Moustahfid, H., Hendrickson, L.C., Arkhipkin, A., Pierce, G.J., Gangopadhyay, A., Kidokoro, H., Markaida, U., Nigmatullin, C., Sauer, W.H., Jereb, P., Pecl, G., de la Chesnais, T., Ceriola, L., Lazar, N., Firmin, C.J., Laptikhovsky, V., 2021. Ecological-fishery forecasting of squid stock dynamics under climate variability and change: review, challenges, and recommendations. Rev. Fish. Scie. Aquacult. 1–36. https://doi.org/10.1080/23308249.2020.1864720.

O'Dor, R., Aitken, J., Jackson, G.D., 2005. Energy balance growth models: applications to cephalopods. Phuket Mar. Biol. Cent. Res. Bull. 66, 329–336.

Olyott, L.J.H., Sauer, W.H.H., Booth, A.J., 2007. Spatial patterns in the biology of the chokka squid, *Loligo reynaudii* on the Agulhas Bank, South Africa. Rev. Fish Biol. Fish. 17, 159–172. https://doi.org/10.1007/s11160-006-9027-5.

Oosthuizen, A., Roberts, M.J., Sauer, W.H.H., 2002. Temperature effects on the embryonic development and hatching success of the squid *Loligo vulgaris reynaudii*. Bull. Mar. Sci. 71, 619–632.

Petrik, C.M., Stock, C.A., Andersen, K.H., van Denderen, P.D., Watson, J.R., 2019. Bottom-up drivers of global patterns of demersal, forage, and pelagic fishes. Prog. Oceanogr. 176, 102124 https://doi.org/10.1016/j.pocean.2019.102124.

Pierce, G., Belcari, P., Bustamante, Paco, Challier, L., González, Á., Guerra, Á., Jereb, Patrizia, Koueta, N., Lefkaditou, Eugenia, Moreno, Ana, Pereira, João, Piatkowski, Uwe, Robin, J.P., Roel, B., Santos, M.B., Santurtun, M., Seixas, Sonia, Shaw, P., Smith, J., Stowasser, G., Villanueva, Roger, Wang, J., Wangvoralak, S., 2010. Cephalopods and climate change 6.1.1 Introduction: climate change and climate variation. In: Pierce, G.J., Allcock, L., Bruno, I., Bustamante, P., González, A., Guerra, A., Jereb, P., Lefkaditou, E., Malham, S., Moreno, A., Pereira, J., Piatkowski, U., Rasero, M., Sánchez, P., Santos, B., Santurtún, M., Seixas, S., Villanueva, R. (Eds.), Cephalopod Biology and Fisheries in Europe. ICES, Copenhagen, Denmark, pp. 86–118.

Pierce, G.J., Valavanis, V.D., Guerra, A., Jereb, P., Orsi-Relini, L., Bellido, J.M., Katara, I., Piatkowski, U., Pereira, J., Balguerias, E., Sobrino, I., Lefkaditou, E., Wang, J., Santurtun, M., Boyle, P.R., Hastie, L.C., MacLeod, C.D., Smith, J.M., Viana, M., González, A.F., Zuur, A.F., 2008. A review of cephalopod–environment interactions in European Seas. Hydrobiologia 612, 49–70. https://doi.org/10.1007/s10750-008-9489-7.

Pope, J.G., Shepherd, J.G., Webb, J., 1994. Successful surf-riding on size spectra: the secret of survival in the sea. Philos. Transact. Royal Soc. London Series B: Biol. Sci. 343, 41–49. https://doi.org/10.1098/rstb.1994.0006.

Roberts, M.J., 2005. Chokka squid (*Loligo vulgaris reynaudii*) abundance linked to changes in South Africa's Agulhas Bank ecosystem during spawning and the early life cycle. ICES (Int. Counc. Explor. Sea) J. Mar. Sci. 62, 33–55. https://doi.org/10.1016/j.icesjms.2004.10.002.

Roberts, M.J., Downey, N.J., Sauer, W.H., 2012. The relative importance of shallow and deep shelf spawning habitats for the South African chokka squid (*Loligo reynaudii*). ICES (Int. Counc. Explor. Sea) J. Mar. Sci. 69, 563–571. https://doi.org/10.1093/icesjms/fss023.

Roberts, M.J., Sauer, W.H.H., 1994. Environment: the key to understanding the South African chokka squid (*Loligo vulgaris reynaudii*) life cycle and fishery? Antarct. Sci. 6, 249–258. https://doi.org/10.1017/S0954102094000386.

Roberts, M.J., van den Berg, M., 2002. Recruitment variability of chokka squid (*Loligo vulgaris reynaudii*) - role of currents on the Agulhas Bank (South Africa) in paralarvae distribution and food abundance. Bull. Mar. Sci. 71, 691–710.

Robin, J.-P., Roberts, M., Zeidberg, L., Bloor, I., Rodriguez, A., Briceño, F., Downey, N., Mascaró, M., Navarro, M., Guerra, A., Hofmeister, J., Barcellos, D.D., Lourenço, S.A. P., Roper, C.F.E., Moltschaniwskyj, N.A., Green, C.P., Mather, J., 2014. Transitions during cephalopod life history: the role of habitat, environment, functional morphology and behaviour. In: Advances in Marine Biology, pp. 361–437. https://doi.org/10.1016/B978-0-12-800287-2.00004-4.

Robinson, J., Popova, E.E., Srokosz, M.A., Yool, A., 2016. A tale of three islands: downstream natural iron fertilization in the Southern Ocean. J. Geophys. Res.: Oceans 121, 3350–3371. https://doi.org/10.1002/2015JC011319.

Rodhouse, P.G., Nigmatullin, ChM., 1996. Role as consumers. Philos. Transact. Royal Soc. London Series B: Biol. Sci. 351, 1003–1022. https://doi.org/10.1098/rstb.1996.0090.

Rodhouse, P.G.K., Pierce, G.J., Nichols, O.C., Sauer, W.H.H., Arkhipkin, A.I., Laptikhovsky, V.V., Lipiński, M.R., Ramos, J.E., Gras, M., Kidokoro, H., Sadayasu, K., Pereira, J., Lefkaditou, E., Pita, C., Gasalla, M., Haimovici, M., Sakai, M., Downey, N., 2014. Environmental effects on cephalopod population dynamics. Adv. Mar. Biol. 67 https://doi.org/10.1016/B978-0-12-800287-2.00002-0, 99–233.

Roel, B.A., 1998. Stock Assessment of the Chokka Squid *Loligo Vulgaris Reynaudii*. University of Cape, Town.

Roel, B.A., Butterworth, D.S., 2000. Assessment of the South African chokka squid *Loligo vulgaris reynaudii*. Fish. Res. 48, 213–228. https://doi.org/10.1016/S0165-7836(00)00186-7.

Roel, B.A., Cochrane, K.L., Butterworth, D.S., 1998. Investigation on the effects of different levels of effort and of the closed season in the jig fishery for chokka squid *Loligo vulgaris reynaudii*. S. Afr. J. Mar. Sci. 19, 501–512. https://doi.org/10.2989/025776198784126935.

Sauer, W.H., Lipiński, M.R., 1991. Food of squid *Loligo vulgaris reynaudii* (Cephalopoda: loliginidae) on their spawning grounds off the Eastern Cape, South Africa. S. Afr. J. Mar. Sci. 10, 193–201. https://doi.org/10.2989/02577619109504631.

Sauer, W.H.H., Downey, N.J., Lipiński, M.R., Roberts, M.J., Smale, M.J., Glazer, J., Melo, Y., 2013. *Loligo reynaudii*, chokka squid. In: Rosa, R., Pierce, G., O'Dor, R. (Eds.), Advances in Squid Biology, Ecology and Fisheries. Nova Science Publishers, New York, NY, pp. 33–72.

Sauer, W.H.H., Melo, Y.C., de Wet, W., 1999. Fecundity of the chokka squid *Loligo vulgaris reynaudii* on the southeastern coast of South Africa. Mar. Biol. 135, 315–319. https://doi.org/10.1007/s002270050629.

Scott, F., Blanchard, J.L., Andersen, K.H., 2014. mizer: an R package for multispecies, trait-based and community size spectrum ecological modelling. Methods Ecol. Evol. 5, 1121–1125. https://doi.org/10.1111/2041-210X.12256.

Shea, E.K., Vecchione, M., 2010. Ontogenic changes in diel vertical migration patterns compared with known allometric changes in three mesopelagic squid species suggest an expanded definition of a paralarva. ICES (Int. Counc. Explor. Sea) J. Mar. Sci. 67, 1436–1443. https://doi.org/10.1093/icesjms/fsq104.

Sheldon, R.W., Prakash, A., Sutcliffe, W.H., 1972. The size distribution of particles in the ocean. Limnol. Oceanogr. 17, 327–340. https://doi.org/10.4319/lo.1972.17.3.0327.

Skákala, J., Ford, D., Brewin, R.J.W., McEwan, R., Kay, S., Taylor, B., Mora, L., Ciavatta, S., 2018. The assimilation of phytoplankton functional types for operational forecasting in the Northwest European shelf. J. Geophys. Res.: Oceans 123, 5230–5247. https://doi.org/10.1029/2018JC014153.

Smale, M., Sauer, W., Roberts, M., 2001. Behavioural interactions of predators and spawning chokka squid off South Africa: towards quantification. Mar. Biol. 139, 1095–1105. https://doi.org/10.1007/s002270100664.

Srokosz, M.A., Robinson, J., McGrain, H., Popova, E.E., Yool, A., 2015. Could the Madagascar bloom be fertilized by Madagascan iron? J. Geophys. Res.: Oceans 120, 5790–5803. https://doi.org/10.1002/2015JC011075.

van Denderen, P.D., Petrik, C.M., Stock, C.A., Andersen, K.H., 2021. Emergent global biogeography of marine fish food webs. Global Ecol. Biogeogr. 30, 1822–1834. https://doi.org/10.1111/geb.13348.

Venter, J.D., Wyngaardt, S. van, Verschoor, J.A., Lipiński, M.R., Verheye, H.M., 1999. Detection of zooplankton prey in squid paralarvae with immunoassay. J. Immunoassay 20, 127–149. https://doi.org/10.1080/01971529909349348.

Vidal, E.A.G., Roberts, M.J., Martins, R.S., 2005. Yolk utilization, metabolism and growth in reared *Loligo vulgaris reynaudii* paralarvae. Aquat. Living Resour. 18, 385–393. https://doi.org/10.1051/alr:2005040.

Vidal, E.A.G., Zeidberg, L.D., Buskey, E.J., 2018. Development of swimming abilities in squid paralarvae: behavioral and ecological implications for dispersal. Front. Physiol. 9 https://doi.org/10.3389/fphys.2018.00954.

von Boletzky, S., 2003. Biology of early life stages in cephalopod molluscs. Adv. Mar. Biol. 143–203. https://doi.org/10.1016/S0065-2881(03)44003-0.

Vovk, A.N., 1985. Feeding spectrum of Longfin squid (*Loligo pealei*) in the north-west Atlantic and its position in the ecosystem. NAFO Sci. Coun. Stud. 8, 33–38.

Waluda, C.M., Rodhouse, P.G., Podesta, G.P., Trathan, P.N., Pierce, G.J., 2001. Surface oceanography of the inferred hatching grounds of *Illex argentinus* (Cephalopoda: ommastrephidae) and influences on recruitment variability. Mar. Biol. 139, 671–679. https://doi.org/10.1007/s002270100615.

Woodworth-Jefcoats, P.A., Polovina, J.J., Dunne, J.P., Blanchard, J.L., 2013. Ecosystem size structure response to 21st century climate projection: large fish abundance decreases in the central North Pacific and increases in the California Current. Global Change Biol. 19, 724–733. https://doi.org/10.1111/gcb.12076.

Yool, A., Popova, E.E., Anderson, T.R., 2013. MEDUSA-2.0: an intermediate complexity biogeochemical model of the marine carbon cycle for climate change and ocean acidification studies. Geosci. Model Dev. (GMD) 6, 1767–1811. https://doi.org/10.5194/gmd-6-1767-2013.

Young, R.E., Harman, R.F., 1988. In: Larva", "paralarva" and "subadult" in cephalopod terminology. Malacologia, 29, pp. 201–207.